Disorder and thermally driven melting of the flux-line lattice in anisotropic layered superconductors

M. Liu, Y. W. He, W. J. Wu, and Y. H. Yang
Department of Physics, Southeast University, Nanjing 210096, China
(Received 26 January 2005; published 21 June 2005)

We develop a three-dimensional flux line lattice model in the layered superconductors, taking into account both long-range magnetic interactions between pancake vortices located in different layers for a single flux line and those between vortices located in the same layer for different flux lines. Using Langevin dynamic simulations, we study the disorder and thermally driven melting transitions from a disentangled Bragg glass (BG) with quasi-long-range order to an entangled amorphous vortex glass (VG) or a vortex liquid (VL) in the disorder strength-temperature phase diagram. Owing to nonmonotonous temperature dependence of the interactions between vortices, the BG-VG melting line exhibit unusual temperature behavior, reproducing the inverse melting phenomenon observed recently on BSCCO crystals.

DOI: 10.1103/PhysRevB.71.224508 PACS number(s): 74.25.Qt, 74.25.Op

I. INTRODUCTION

In highly anisotropic superconductors, the flux-line lattice (FLL) can be built up by superposing the contributions of stacks of two-dimensional (2D) pancake vortices.[1–3] It has been widely accepted that at low temperatures and low magnetic fields, these vortices, which interact both magnetically and through Josephson coupling, align into a 3D linelike elastic lattice without dislocations, which is called the quasi-long-range ordered Bragg glass (BG) phase. However, undergoing a thermally driven or a disorder driven condition, the FLL may melt into an entangled vortex liquid (VL) or an entangled vortex solid (VG) phase. The differece between VG and VL phases is that the zero resistivity is kept for the former and not for the latter.

Recently, Avraham *et al.*[4] reported an unusual first-order "inverse melting" behavior of the lattice formed by magnetic flux lines, using local magnetization measurements combined with a vortex "shaking" technique on the $Bi_2Sr_2CaCu_2O_8$ (BSCCO) crystals. They found that, in the field-temperature phase diagram, the first-order transition (FOT) line does not terminate at T_{cp}, but continues down to a lower temperature. The slope of the FOT line changes sign at T_{cp}. While the melting line above T_{cp} has a negative slope, characterizing the thermal driven first-order phase transition; the melting line below T_{cp} exhibits a positive slope and has a different underlying nature, which is a disorder-driven BG-VG transition. In such a BG-VG transition, the vortex lattice from an ordered phase transforms into an disordered amorphous phase upon cooling. This finding leads to several important results. One is that the disorder-driven transition at the second magnetization peak is of first order. This result is consistent with recent results based on Josephson plasma resonance studies,[5] transport measurements,[6] neutron scattering experiments on Nb,[7] as well as several numerical simulations[8–11] and theoretical studies.[12,13] Recently, the presence of metastable states and superheating/supercooling effects strongly suggested that the BG-VG transitions in different materials are first order in nature,[11] and this transition is associate with the peak effect in the critical current in experimental. It then follows that the BG-VL melting line and BG-VG transition line are two manifestations of the same FOT. The disorder-driven transition should be a universal phenomenon and is apparently at the heart of the ubiquitous peak effect in low-T_c superconductors.[6] Another result is that the phase boundary between BG and VG phases is upturned at intermediate temperature region. Similar temperature dependence of the BG-VG transition line was also reported in other layered superconductors.[14–17] It was argued[4] that the disorder-driven transition arises from the competition between the elastic energy of lattice and the vortex pinning energy. At the intermediate temperature regime, thermal fluctuations reduce the pining energy, resulting in an upturn of the BG-VG transition line.

In recent theoretical and numerical studies on the phase diagram of vortex states,[8–10,12,13] the obtained phase boundaries between BG and VG phases are almost independent of temperature, and the inverse melting behavior has not been understood. It is highly desirable to find out a reasonable explanation for this disagreement in melting behavior between existing experiments and theories. In this paper, we do not want to study the FOT nature in high-T_c superconductors, but instead focus on the temperature dependence of the BG-VG phase border in the vortex phase diagram. Taking into account long-range magnetic interactions between pancake vortices located in different layers for a single flux line and those between vortices located in the same layer for different flux lines, we develop a 3D rigid flux line lattice model to simulate the disorder strength-temperature phase diagram. It is found that the temperature dependence of the in-plane penetration depth makes the magnetic interactions between vortices exhibit nonmonotonic temperature behavior. The present simulation can provide a qualitative explanation for the inverse melting behavior observed experimentally.

II. MODEL

We study a 3D flux line lattice system considering the random pinning, thermal fluctuations, and long-range mag-

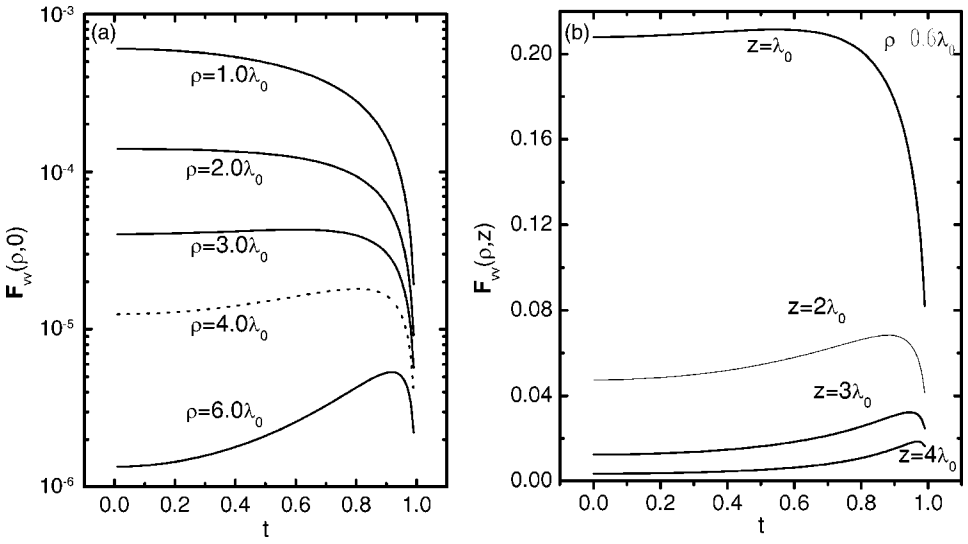

FIG. 1. Temperature dependence of (a) the repulsive force $F_{vv}(\rho,0)$ for different values of ρ; (b) the attractive force $F_{vv}(\rho,Z)$ for different values of Z.

netic interactions between all pancake vortices. In this line-like lattice, each flux line is composed of L_z vortices and each layer contains N_v vortices distributed in a square lattice and N_p pinning centers distributed randomly. The pancake vortices in a layer are modeled as repulsive point particles. With no driving, the overdamped equation of motion for the ith vortex is given by $\eta \mathbf{v}_i = \mathbf{F}_p + \mathbf{F}_{th} + \mathbf{F}_{vv}$.[18] $\mathbf{F}_p$ is the pinning force. The point pinning potential is modeled by a Gaussian potential well with decay length as R_p, and the pinning strength is described by $F_{p0}f_0$ with f_0 as the unit of force. As pointed out in Refs. 8, 9, and 18, the effective randomness strength may be assumed to increase with increasing magnetic field, so that an H-T diagram may be replaced with an $F_{p0}f_0$-T diagram. The thermal noise force $\mathbf{F}_{th}$ is assumed to be a Gaussian white noise. $F_{th0}(T)f_0$ stands for the intensity of the thermal fluctuation force, which is proportional to the square root of temperature.

In highly anisotropic superconductors, both the in-plane and out-of-plane pancake interactions are long range, and the Josephson coupling may be neglected as a reasonable approximation.[1] According to the magnetic interaction model, the vortex-vortex interaction $\mathbf{F}_{vv}$ includes two parts:[1,2,11,19,20] the repulsive interaction between two pancake vortices located in the same plane, and the attractive interaction between two vortices located in different layers but along the same line. We first consider the in-plane repulsive interaction due to the overlap of magnetic vortex field.[2,18] In the present model each vortex in the plane represents a segment of rigid flux line with finite length. As a result, the in-plane pancake vortex system under consideration are not a simple 2D model, but contains important 3D effects. From the London theory, the in-plane repulsive potential between two vortices located at $\mathbf{r}_i, z_l$ and $\mathbf{r}_j, z_l$ is given by $E_{vv}(\rho_{i,j},0) = (L\phi_0^2/4\pi\mu_0\lambda_T^2)K_0(\rho_{i,j}/\lambda_T)$. Here $K_0(z)$ is the modified Bessel function of the third kind and λ_T is the in-plane superconducting penetration depth. $\rho_{i,j} = |\mathbf{r}_i - \mathbf{r}_j|$ is the distances between the two pancakes in cylindrical coordinates. The intervortex repulsive force on vortex i is equal to the derivative of the interacting potential,

$$\mathbf{F}_{vv}(\rho_{i,j},0) = \frac{F_{vv0}f_0}{\lambda_T^3} K_1\left(\frac{|\rho_{i,j}|}{\lambda_T}\right)\frac{\mathbf{r}_{i,j}}{r_{i,j}}, \tag{1}$$

where $F_{vv0}f_0$ stands for the intensity of the interaction between vortices. The interacting force depends on temperature via the temperature-dependent penetration depth $\lambda_T = \lambda_0/\sqrt{1-t^2}$, where λ_0 is the in-plane penetration depth at zero temperature and taken as the unit of length, and $t = T/T_c$. Owing to a competition between the decreased prefactor and sharply increased Bessel function with temperature, $F_{vv}(\rho,0)$ exhibits unusual temperature dependence, as shown in Fig. 1(a). We can see that for the spacing between vortices $\rho < 4\lambda_0$, the interacting force decreases monotonously with increasing temperature. For $\rho \geqslant 4\lambda_0$, however, it first increases with temperature and has a big drop near T_c.

The attractive interactions between out-of-plane vortices are very important for the 3D vortices system forming a rigid line lattice in a disordered superconductor. According to the model proposed by Clem[1] and an effective approach,[11,19,20] the straight vortex line can be built up by superposing the contributions of stacks of 2D pancake vortices through the long-range magnetic interactions along the line direction. The attractive interaction between two pancake vortices at $\mathbf{r}_i, z_l$, and $\mathbf{r}_j, z_k$, in a single flux line but different layers is given by,[1,11,19,20]

$$\mathbf{F}_{vv}(\rho_{i,j},z_{l,k}) = -S_m\frac{dA_{vv0}}{2\lambda_T\rho_{i,j}}\left[\exp\left(-\frac{|Z_{l,k}|}{\lambda_T}\right) - \exp\left(-\frac{\sqrt{\rho_{i,j}^2+Z_{l,k}^2}}{\lambda_T}\right)\right]\frac{\mathbf{r}_{i,j}}{r_{i,j}}. \tag{2}$$

Here S_m is the interlayer coupling parameter and d is the thickness of superconducting layers. In this magnetic interaction model, we do not consider the interlayer Josephson coupling with a short force range of the coherence length scale, and here $Z_{l,k} = |Z_l - Z_k|$ is treated to be of long range. In Ref. 1, the above equation was deduced on the assumption that the spatial variation of z is on the scale of $\lambda_\parallel$ and larger,

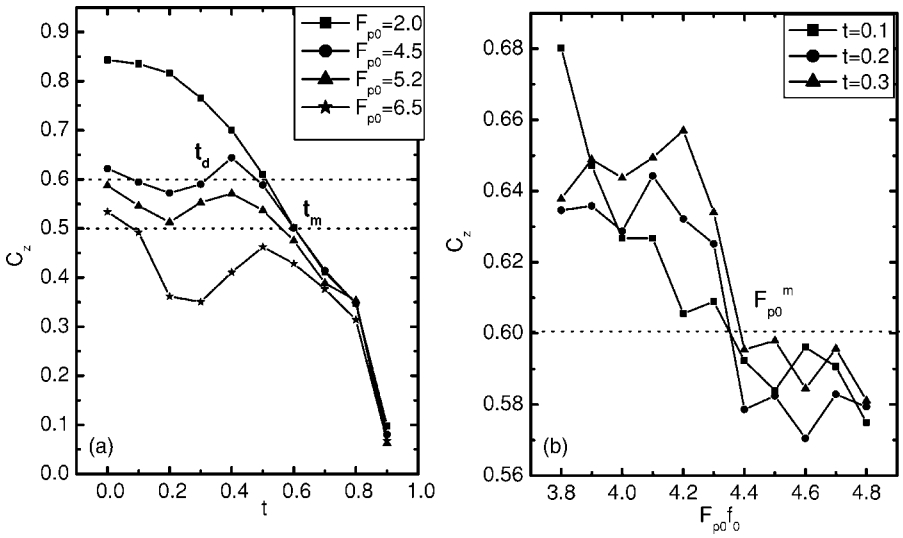

FIG. 2. Correlation function C_z as functions of (a) temperature t for different pinning strength F_{p0}; (b) disorder strength $F_{p0}f_0$ for different t.

so we take the value of the stacking periodicity length $s=Z_{l,l\pm1}$ as the λ_0 scale. The minus sign in the prefactor indicates that the interplane magnetic force along the $\mathbf{r_{i,j}}$ direction is attractive. This attractive force varies with ρ first increasing linearly until $\rho \simeq \lambda_0$ and then decrease slowly, exhibiting an elastic attractive force which is favorable to the coaxial alignment of vortices. In this work we consider the in-plane penetration depth divergence with increasing temperature near T_c, $F_{vv}(\rho,Z)$ also exhibits an unusual temperature dependence, as shown in Fig. 1(b). We can see that $F_{vv}(\rho,Z)$ first increases with increasing t and then decreases at higher temperature near T_c. The unusual temperature behavior of in-plane and out-of-plane magnetic interactions is found to be the key factor, causing an upturn of the BG-VG phase border.

Since the transition from alignment to entanglement of rigid flux lines and the decoupling between the pancake vortices in different layers occur almost simultaneously, we use the loss of coherence or the decoupling between the layers as the criterion of melting transition of the FLL system,[11,19,20] in which the rigid flux lines are entangled (or decoupled) into disordered 2D vortex pancakes in the absence of coherence between the layers. The correlation function in the c direction is defined by $C_z=1-\langle\Theta(a_0-|\mathbf{r}_{i,l}-\mathbf{r}_{i,l+1}|)|\mathbf{r}_{i,l}-\mathbf{r}_{i,l+1}|2/a_0\rangle$ where a_0 is the in-plane vortex lattice constant. We will choose a constant value of the correlation function, $C_z=C_0$, as the transition point, $C_z>C_0$, indicating an ordered phase and $C_z<C_0$ a disordered phase. The choice of C_0 is mainly determined by two factors. First, C_z should have a visible drop at C_0 and then decrease to zero, as shown in Fig. 2(a). Next, on the both sides of C_0 there are qualitatively different ordered and disordered characteristics, as shown in the insets of Fig. 3. For weak pinning strength, e.g., $F_{p0}=2.0$ in Fig. 2(a), it is found that for $1.0\geqslant C_z>0.5$, the pancakes are aligned into rigid lines and the FLL system is regarded as a coupled BG phase with quasi-long-range order (shown in the lower left inset of Fig. 3). For $C_z<0.5$, corresponding to the higher temperature case, the FLL system may be regarded as a decoupled disordered liquid phase (shown in the lower right inset of Fig. 3). Evidently, $C_0=0.5$ is not the only choice, the other choice deviated from $C_0=0.5$, provided that it is in a reasonable range, will not change the qualitative results obtained below.

For stronger pinning strength and at lower temperatures, the criterion of BG-VG transition is somewhat different from that of the BG-VL one. In this case, the disorder-driven force is the random pinning interaction rather than the thermal fluctuations. In such a disordered VG phase, the decoupled pancakes in neighboring planes still remain in a short-range order, and the "flux lines" remain but are entangled, so that the FLL system may be regarded as a entangled solid with zero resistivity kept (shown in the upper left inset of Fig. 3). As a result, for the BG-VG transition, C_z is chosen to be a lower value such as in a range of $0.6>C_z>0.5$.

III. RESULTS AND DISCUSSIONS

Using numerical simulations, we investigate the melting transition of an ordered FLL by changing temperature t and the randomness strength $F_{p0}f_0$. We normalize length scales by the in-plane penetration length at zero temperature λ_0, and take $a_0=4\lambda_0$, $R_p=0.5\lambda_0$, and $d=0.01\lambda_0$. For the nearest-neighbor layers, the interlayer coupling parameter $S_m=0.18$. For the second nearest-neighbor layers, $S_m=13.33$. Other parameters used are $L_z(=20)$, $N_v(=81)$, $N_p(=162)$, $F_{th0}f_0=0.36$, $F_{vv0}f_0=0.05$, and $dA_{vv0}=10$. The periodic boundary condi-

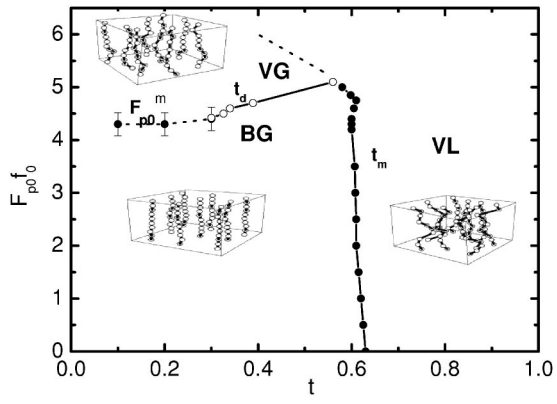

FIG. 3. Phase diagram of vortex lattice in $F_{p0}f_0$-t plane.

tions both in the plane and along the c direction are applied. We also simulate vortex systems of different sizes, by keeping both densities of vortices and pinning centers unchanged. The simulated results are found insensitive to the choice of the sample size, indicating that the present calculations are reliable.

We first study the temperature-driven melting transition by slowly increasing temperature of the vortex system with the pinning strength fixed. In the present simulations, the initial configuration of the FLL system is set to be a set of rigid lines distributed uniformly in a square lattice, and 2×10^5 Monte Carlo steps are used to let the vortices approach their equilibrium distribution. The calculated results for C_z as functions of t for different $F_{p0}f_0=2.0,4.5,5.2,6.5$ are plotted in Fig. 2(a). It is found that, for small pinning strengths (e.g., $F_{p0}f_0=2.0$), the FLL remains BG phase with $C_z>0.5$ at lower temperatures; as the temperature rises to a critical value $t_m(=0.6)$, C_z has an abrupt drop towards zero, indicating a transition from the BG phase to VL phase. This melting transition at t_m is mainly thermal driven, because the pinning strength remains unchanged. For a larger pinning strength (e.g., $F_{p0}f_0=4.5$), the situation is quite different. In addition to the VL phase at higher temperatures $t>t_m(=0.6)$, there exists another disordered VG phase at low temperatures $t<t_d(=0.33)$ due to disorder-induced fluctuations. At the intermediate temperatures between t_d and t_m, the value of the correlation function has an unusual hump $C_z>0.6$, indicating the appearance of a new BG state. It follows that in this temperature regime the ordering effect due to vortex-vortex interactions prevails over disorder effects due to pinning and thermal fluctuations, resulting in a reentrant phenomenon at t_d. For strong pinning strength (e.g., $F_{p0}f_0=5.2$ and 6.5), the melting temperature is reduced to $t_m=0.55$ and 0.1. From the two curves we can see that at low temperatures $t<t_m$, the FLL system is in the VG phase with the values of $C_z<0.6$ and keeps them between 0.5-0.6; with increasing temperature ($t>t_m$), the FLL system melts into the VL phase.

We also calculate C_z as functions of $F_{p0}f_0$ at low temperatures $t=0.1,0.2,0.3$, the calculated results plotted in Fig. 2(b). It is found that when F_{p0} increases to certain critical value (F_{p0}^m), C_z decreases below 0.6; and after then it remains unchanged or decreases slowly. It follows that the BG-VG transition of the FLL system is of disorder-driven origin. In Fig. 2(b), $F_{p0}^m f_0\sim4.435,4,435,4.439$ for $t=0.1,0.2,0.3$, respectively. The correlation function C_z in Fig. 2(b) seems to have no visible singularity at the BG-VG transition point F_{p0}^m. In the present BG-VG transition the disorder phase is not the thermally driven liquid, but the disorder-driven amorphous phase due to the pinning centers distributed randomly. While in the thermal-driven transition, the correlation function decreases rapidly with increasing temperature, exhibiting a singularity; in the disorder-driven BG-VG transition, its decrease with the pinning strength is relatively small and it tends constant when the pancakes are completely pinned by the quenched disorder. This result is related to the experimental fact[4,14–16] that while the melting transition into a liquid vortex state is manifested by a discontinuous jump in the reversible magnetization, the solid-solid transition into an entangled vortex state is manifested by the appearance of a second magnetization peak with pronounced features such as onset, kink, or peak. In addition, the present calculated results are found to have significant history and memory effects near the transition line F_{p0}^m, indicating that this BG-VG transition is close related to the nature of a first-order phase transition.

From all the calculated results of C_z by scanning pinning strength and temperature, we construct a steady-state phase diagram on the $F_{p0}f_0-t$ plane, as shown in Fig. 3. Here the solid line with solid circles and negative slope indicates the BG-VL phase border which is an assembly of t_m vs F_{p0} obtained above. The solid line with open circles and positive slope indicates the BG-VG phase border which is an assembly of t_d vs F_{p0}. The dashed line with solid circles and bars represents the BG-VG phase border which consists of F_{p0}^m vs t. The upper dashed line is drawn by t_m vs F_{p0}, and represents the transition between VG and VL phases. Both solid and dashed lines in Fig. 3 construct a complete phase diagram that consists of three sectors. The right boundary between BG and VL phases is a result of competition mainly between the intervortex interactions and thermal fluctuations. At the same time, random pinning provides a little of disorder factor, making this sector of boundary exhibit a negative slope. The low-temperature sector is the boundary between BG and VG phases, which is a result of competition mainly between the intervortex interactions and random pinning. For weak pinning strength the vortex lattice remains its ordered BG structure, as the pinning strength is increased strong enough, disorder caused by random pinning drives a transition of vortex lattice from the BG to VG phase, and results in a highly pinned phase of entangled vortices. At low temperatures, thermal fluctuations have little effect on the phase transition, and this sector of phase boundary is almost parallel to the temperature axis.

At intermediate temperatures, the solid line is still the boundary between BG and VG, but it has a positive slope. There is a hump of the transition line near the crossed temperature between t_m and t_d, indicating an appearance of reentering the BG state and the inverse melting behavior. This unusual behavior stems from a competition between ordering and disorder. As shown in Fig. 1, both in-plane and out-of-plane interacting forces between the vortices may be enhanced by increasing the temperature in the intermediate temperature regime. If the the temperature-enhanced interacting force may prevail over the disordered pinning effect and thermal fluctuations, the reentering BG state will appear. The reentering BG state obtained in the present simulation provides a qualitative explanation for the inverse melting behavior observed experimentally. In the present calculations, however, if the intervortex interactions are assumed to be independent of temperature, there will be neither hump of disorder-driven transition line nor inverse melting behavior. It appears that the inverse melting behavior arises from the temperature-enhanced interactions between vortices rather than the reduction of pinning effects by thermal fluctuations.[4] From the present model, it follows that the inverse melting phenomenon does exist in the vortex lattice of the high-T_c superconductors, even though it is not very easy to be observed.

ACKNOWLEDGMENTS

This work was supported by the National Natural Science Foundation of China under Grants No. 10174011 and No. 10274008, and the Natural Science Foundation of Jiangshu of China under Grant No. BK2002050. Y. H. Yang would like to acknowledge the support of the Program for New Century Excellent Talents in the University of China.

[1] J. R. Clem, Phys. Rev. B **43**, 7837 (1991).
[2] E. H. Brandt, Rep. Prog. Phys. **58**, 1465 (1995); Physica C **369**, 10 (2002); G. P. Mikitik and E. H. Brandt, Phys. Rev. B **64**, 184514 (2001).
[3] A. E. Koshelev, Phys. Rev. B **68**, 094520 (2003).
[4] N. Avraham, B. Khaykovich, Y. Myasoedov, M. Rappaport, H. Shtrikman, D. E. Feldman, T. Tamegai, P. H. Kes, M. Li, M. Konczykowki, C. J. van der Beek, and E. Zeldov, Nature (London) **411**, 451 (2001).
[5] M. B. Gaifullin, Y. Matsuda, N. Chikumoto, J. Shimoyama, and K. Kishio, Phys. Rev. Lett. **84**, 2945 (2000).
[6] Y. Paltiel, E. Zeldov, Y. Myasoedov, M. L. Rappaport, G. Jung, S. Bhattacharya, M. J. Higgins, Z. L. Xiao, E. Y. Andrei, P. L. Gammel, and D. J. Bishop. Phys. Rev. Lett. **85**, 3712 (2000).
[7] S. R. Park, S. M. Choi, D. C. Dender, J. W. Lynn, and X. S. Ling, Phys. Rev. Lett. **91**, 167003 (2003).
[8] Y. Nonomura and X. Hu, Phys. Rev. Lett. **86** 5140 (2001).
[9] P. Olsson and S. Teitel, Phys. Rev. Lett. **87** 137001 (2001).
[10] S. Ryu, A. Kapitulnik, and S. Doniach, Phys. Rev. Lett. **77**, 2300 (1996).
[11] C. J. Olson, C. Reichhardt, R. T. Scalettar, G. T. Zimanyi, N. Grønbech-Jensen, Phys. Rev. B **67**, 184523 (2003); C. J. Olson *et al.* Physica C **384**, 143 (2003)
[12] G. P. Mikitik and E. H. Brandt, Phys. Rev. B **68**, 054509 (2003); **64**, 184514 (2001).
[13] J. Kierfeld and V. Vinokur, Phys. Rev. B **61**, R14 928 (2000).
[14] D. Pal, S. Ramakrishnan, A. K. Grover, D. Dasgupta, and B. K. Sarma, Semicond. Sci. Technol. **15**, 258 (2002).
[15] Y. Radzyner, A. Shaulov, Y. Yeshurun, I. Felner, K. Kishio, and J. Shimoyama, Phys. Rev. B **65**, 100503(R) (2002).
[16] Y. Radzyner, S. B. Roy, D. Giller, Y. Wolfus, A. Shaulov, P. Chaddah, and Y. Yeshurun, Phys. Rev. B **61**, 14 362 (2000).
[17] M. B. Maple, B. J. Taylor, S. Li, N. A. Frederick, V. F. Nesterenko, and S. S. Indrakanti, Physica C **387**, 131 (2003).
[18] J. Wang, Z. G. Zhao, M. Liu, D. Y. Xing, and J. M. Dong, Europhys. Lett. **65**, 89 (2004).
[19] A. B. Kolton, D. Domínguez, C. J. Olson, and N. Grønbech-Jensen, Phys. Rev. B **62**, R14 657 (2000).
[20] C. J. Olson, C. Reichhardt, and V. M. Vinokur, Phys. Rev. B **64**, 140502(R) (2001); C. J. Olson *et al.*, Physica C **384**, 143 (2003).